AN EXPERIMENTAL STUDY OF TURBULENT WAKE/BOUNDARY LAYER MIXING FLOWS

L J Johnston
Aircraft Research Association Ltd
Bedford, England
and
H P Horton
Department of Aeronautical Engineering
Queen Mary College, University of London

Abstract

In order to design efficient high-lift systems, the flow around multi-element aerofoils must be understood. Of particular importance is the interaction between the viscous layers developing on the various aerofoil elements. For example, the mixing of the wake from a leading-edge slat with the main element boundary layer can play a crucial role in determining the maximum lift attainable from the high-lift system. The present work was undertaken to study in detail this wake/boundary layer mixing process in two-dimensional flow. A preliminary study concentrated on the mixing of a symmetric aerofoil wake with a flat plate boundary layer. The second part of the experimental programme considered a two-element aerofoil system in a wing/leading-edge slat configuration. The geometry of the aerofoil system was chosen so as to produce a strong interaction of the viscous layers, leading to eventual flow separation. Measurements included traverses through the viscous layers at a large number of stations. Hot-wire anemometry was used to measure Reynolds normal and shear stress distributions. The results indicate that simple algebraic turbulence models, based on self-similar flow development, become inadequate in the presence of strong wake/boundary layer interactions. A calculation method using modelled turbulence transport equations gives good predictions for the present flows. Such a turbulence model appears to be the best approach to the prediction of the flow development around practical high-lift systems.

1 Introduction

Figure 1 indicates the range of viscous flow phenomena that occur on a multi-element aerofoil section operating close to $C_{L_{max}}$. The leading-edge slat element is highly loaded, and supercritical flow may be present for freestream Mach numbers as low as 0.2. There are separation bubbles behind the slat hook and in the flap cove region. These are due to the sharp edges dictated by the geometrical constraint which requires the slat and flap to retract and form a smooth section.

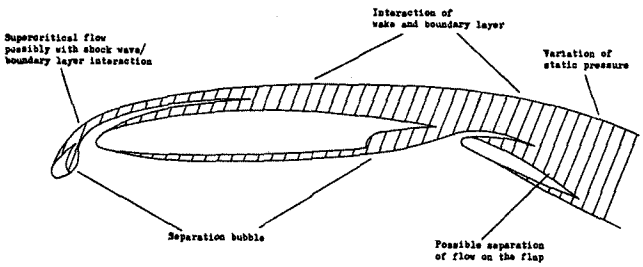

FIGURE 1

The wakes from upstream elements mix with the boundary layers on the elements immediately downstream, to form thick viscous layers. The development of these viscous layers is affected significantly by flow curvature when the high-lift system is operating near to maximum lift conditions. Flow separation may be present on one or more of the aerofoil elements. However, the abrupt loss of lift associated with the final stall is not due to flow separation from the flap element. As indicated by Petrov,[1] the stall is precipitated by reverse flow in the wakes developing above the main aerofoil and flap elements. In fact, the flow on the flap remains fully-attached throughout the stall, as demonstrated by Seetharam and Wentz.[2] The development of the wakes, together with any associated mixing with adjacent boundary layers, thus plays a crucial role in determining the maximum lift attainable from a high-lift system.[3]

The present work is concerned with turbulent wake/boundary layer mixing in two-dimensional, incompressible flow. Figure 2 shows what may be termed the multi-layer representation of the merging viscous layers, composed of a wall layer and two half-wake layers. Such a representation has been used by Irwin[4] and Goradia[5] as the basis of integral calculation methods. Self-similar mean velocity profiles are used to represent each of the layers. When substituted into the boundary layer equations, a set of ordinary differential equations is obtained which describe the development of the mean velocity and length scales characterising the flow, Figure 2. The integral method approach is not easily extendable to more complex flow situations, such as the multiple wake/boundary layer mixing that occurs on double- or triple-slotted flap configurations. A calculation method which solves the boundary

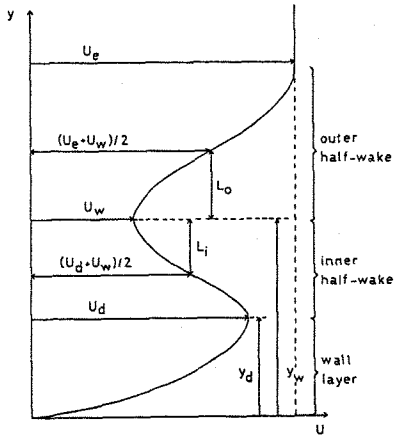

FIGURE 2

layer equations in differential form is preferable in these situations. Such a method requires an explicit turbulence model to close the set of governing flow equations. Finally, it should be mentioned that the thick viscous layers resulting from the wake/boundary layer mixing may be in strict violation of the boundary layer approximation.

The purpose of the work to be described below was to obtain measurements of mean flow and turbulence quantities in wake/boundary layer mixing flows. Such measurements have been made in the past by workers such as Pot,[6] Barjo et al,[7] Zhou and Squire,[8] Brune and Sikavi.[9] However, the present study was aimed at a more detailed analysis of the measurements than had hitherto been attempted.[10] In particular, the turbulence data were assessed for their implications as regards the modelling of the merging viscous layers in a practical calculation method. The multi-layer representation of Figure 2 was used as a convenient framework within which to conduct this analysis.

II Experimental Arrangement for Case (a)

This preliminary experiment considered the simplest possible flow configuration, that of a flat plate turbulent boundary layer mixing with an initially symmetric turbulent wake under nominally zero pressure gradient conditions, Figure 3. The boundary layer developed on the lower surface of a large flat plate, 2.39 m in length and 0.762 m span. The reference length c for the flow was taken to be 1.3 m, corresponding to the actual length of plate within the working section of the wind tunnel (the remainder extending into the diffuser section). The wake was produced by a symmetric section aerofoil of chord c_s = 0.305 m and thickness/chord ratio of 0.14. The aerofoil was positioned with its trailing-edge in line with the leading-edge of the plate, and displaced 11.5 mm from the plate surface. The experiment was conducted in a low speed blowdown wind tunnel, at a reference freestream velocity U_o of 17.9 m/s and Reynolds number of 1.23×10^6 per metre. Hot-wire probes, in conjunction with a constant temperature anemometry system, were used to measure mean velocities and Reynolds stresses. The skin friction distribution on the flat plate was measured using the surface pitot probe technique.

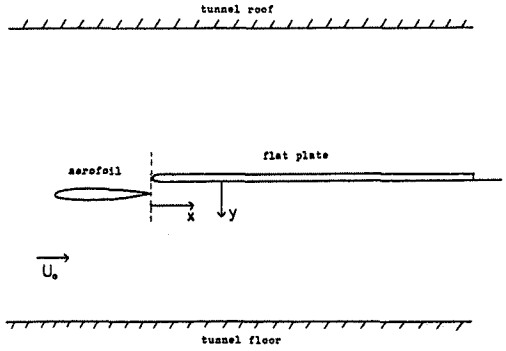

FIGURE 3

III Results for Case (a)

Figure 4a shows the development of the mean velocity profile, measured using a single-wire probe. Profiles of shear stress $-\overline{uv}$ and turbulent kinetic energy k are shown in Figure 4b and c, these being measured using an X-wire probe. k is defined as

$$k = \tfrac{1}{2}(\overline{u^2} + \overline{v^2} + \overline{w^2}). \qquad (1)$$

The lateral Reynolds normal stress $\overline{w^2}$ was not measured, and so was taken to be equal to $\tfrac{1}{2}(\overline{u^2} + \overline{v^2})$ when evaluating k. Figure 5 shows the integral thicknesses for the total viscous layer, together with the skin friction distribution on the flat plate. These measurements were inserted into the momentum integral equation, which was integrated in the downstream direction. The resulting momentum balance indicated the flow to be accurately two-dimensional.

The measurements were examined on the basis of the multi-layer representation of Figure 2. This indicated that the development of the outer half-wake layer appeared to be unaffected by the merging taking place closer to the plate surface. The mean velocity and length scales of a self-preserving wake of small velocity deficit develop, in zero pressure gradient, as[11]

$$\frac{\Delta U_o}{U_e} = \frac{U_e - U_w}{U_e} \propto \left(\frac{x - x_o}{c_s}\right)^{-\frac{1}{2}} \qquad (2)$$

and

$$\frac{L_o}{c_s} \propto \left(\frac{x - x_o}{c_s}\right)^{\frac{1}{2}}, \qquad (3)$$

where x_o is the virtual origin of the wake. Figure 6 shows the development of these scales for the outer and inner half-wake layers (with $\Delta U_i = U_d - U_w$ for the inner half-wake). The outer half-wake does indeed develop in a self-preserving manner, with a virtual origin x_o/c_s of -0.19. ΔU_i and L_i both decay to zero as the inner half-wake merges with the wall layer, and so cannot develop a self-preserving form. Further analysis of the data for case (a) is presented in Reference 12, which also contains the data in tabular form.

IV Experimental Arrangement for Case (b)

The second part of the experimental programme considered a configuration more representative of flow conditions on a multi-element aerofoil high-lift system. However, the choice of a suitable configuration was constrained by the size of the wind tunnel working section (the same as used for case (a)), which precluded the use of a large aspect ratio model. It is usual to use sidewall boundary layer control and large aspect ratio models when testing wing/trailing-edge flap configurations. Figure 7a shows the configuration chosen, consisting of two symmetric section aerofoils in a wing/leading-edge slat arrangement. The main aerofoil chord c was 0.762 m and the slat chord c_s was 0.254 m. Both aerofoils had the same section, with a thickness/chord ratio of 0.12 and a span of 0.8128 m. The incidence angle was 9°, with the slat element deflected 14° relative to the chordline of the main aerofoil. The slat gap and overlap of 0.025c and zero respectively were chosen to give a strong interaction between the wake and

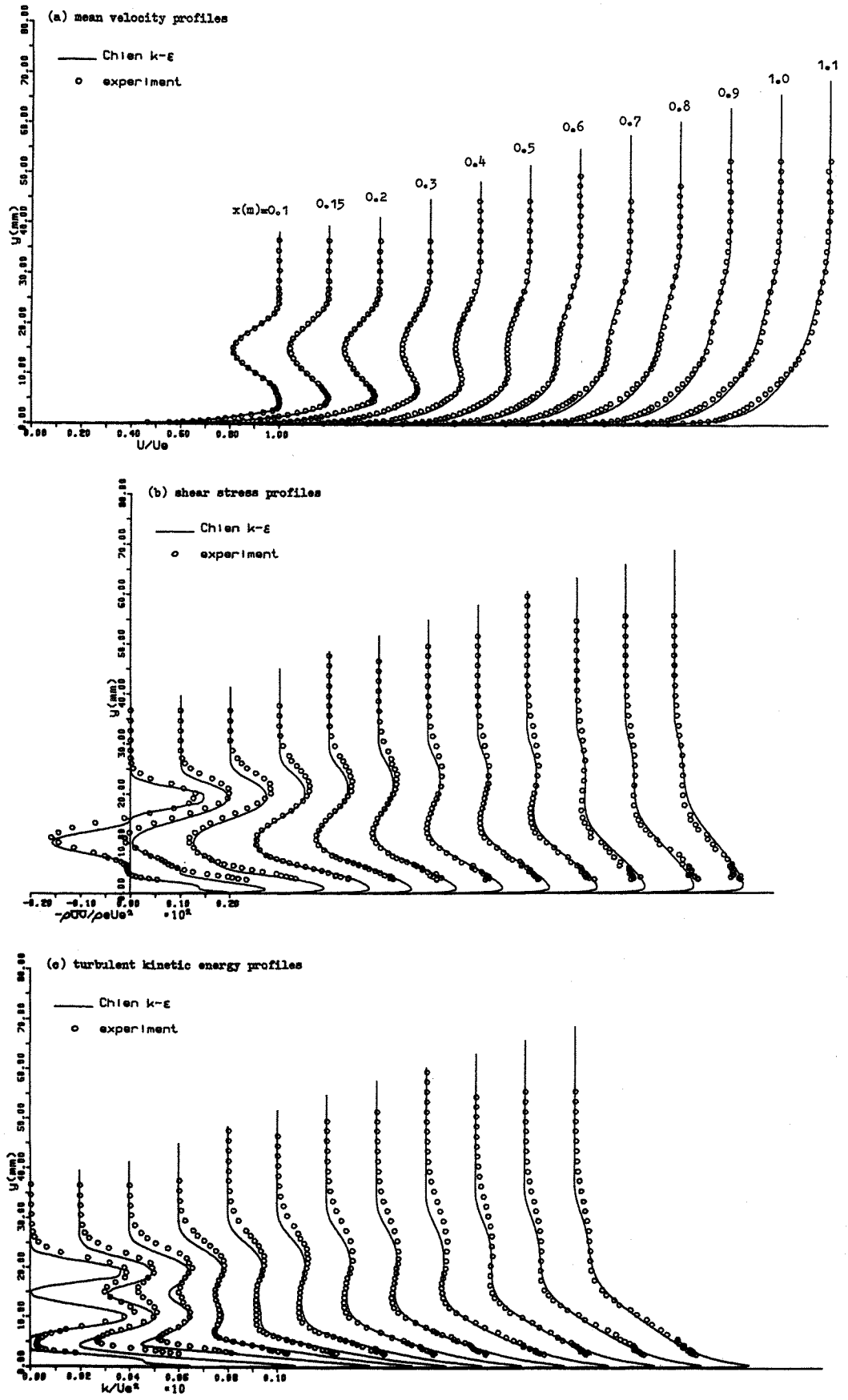
(a) mean velocity profiles
Chien k-ε
experiment
x(m)=0.1
0.15
0.2
0.3
0.4
0.5
0.6
0.7
0.8
0.9
1.0
1.1
y(mm)
U/Ue
(b) shear stress profiles
Chien k-ε
experiment
y(mm)
-ρUV/ρeUe²
(c) turbulent kinetic energy profiles
Chien k-ε
experiment
y(mm)
k/Ue²

FIGURE 4

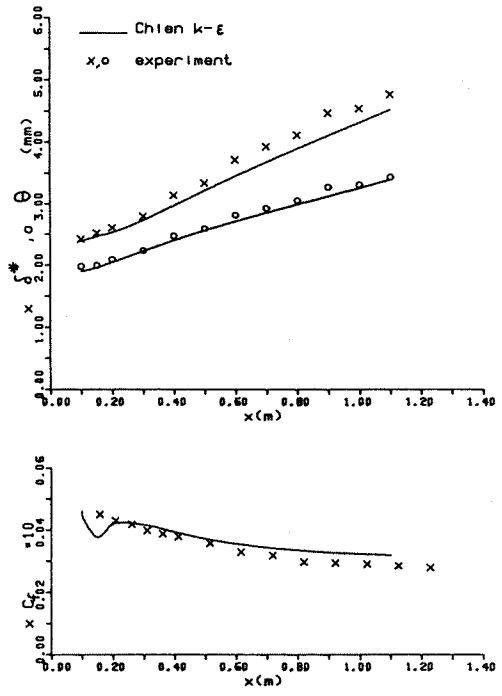

FIGURE 5

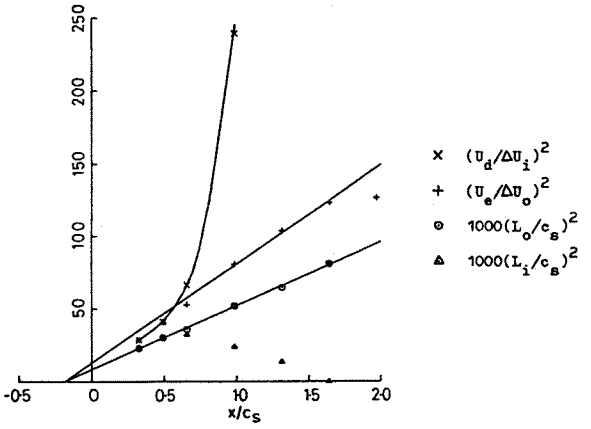

FIGURE 6

boundary layer, leading to flow separation very close to the main aerofoil trailing-edge.

The surface pressure distributions of the two aerofoils are shown in Figure 7b. Note the high level of wind tunnel blockage, as indicated by the main aerofoil trailing-edge pressure. No attempt was made to simulate free air conditions, since the primary concern of the experiment was the viscous flow development. Oil and titanium oxide flow visualisation, together with a momentum balance, indicated the flow to be adequately two-dimensional along the centrespan station, without the need to resort to sidewall boundary layer control. The freestream velocity U_0 was 23 m/s, giving a Reynolds number of 1.21×10^6 based on c.

V Results for Case (b)

Pitot and static pressures were measured across the merging viscous layers at 12 stations. Figure 8a shows the resulting mean velocity profiles. The static pressure profiles are plotted in terms of an equivalent inviscid velocity U_i, where $U_i/U_0 = \sqrt{(1 - C_{ps})}$ and C_{ps} is the local static pressure coefficient. U and U_i are scaled with U_{iw}, the equivalent inviscid velocity at the surface. The profiles of U_i indicate the presence of significant static pressure gradients across the viscous layers. In the leading-edge region this is, essentially, a surface curvature effect with $U_i/U_{iw} < 1$. However, $U_i/U_{iw} > 1$ in the trailing-edge region, which can be interpreted as a streamline curvature effect due to the streamlines diverging from the surface as the flow approaches separation.

Profiles of shear stress and turbulent kinetic energy are shown in Figure 8b and c. These were measured using an X-wire probe, and for this case, all three Reynolds normal stresses were measured. Figure 9 shows the development of the integral thicknesses for the total viscous layer and the skin friction on the main aerofoil (note that the definitions of δ^* and θ include the effects of the static pressure gradients normal to the surface). The skin friction coefficient extrapolates to zero at the trailing-edge of the main aerofoil, indicating incipient flow separation.

The mean velocity profiles are plotted in the semi-logarithmic form appropriate to ordinary turbulent boundary layers in Figure 10. The wall layer conforms to the law-of-the-wall

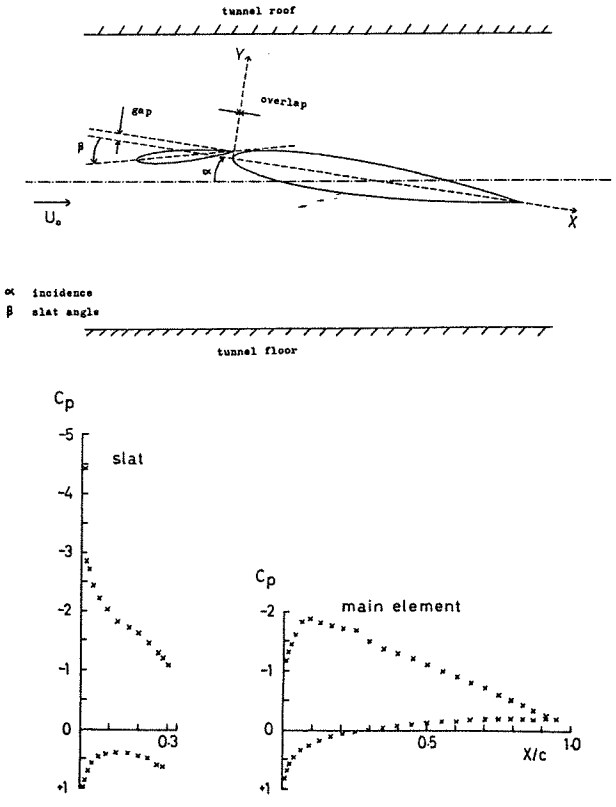

FIGURE 7

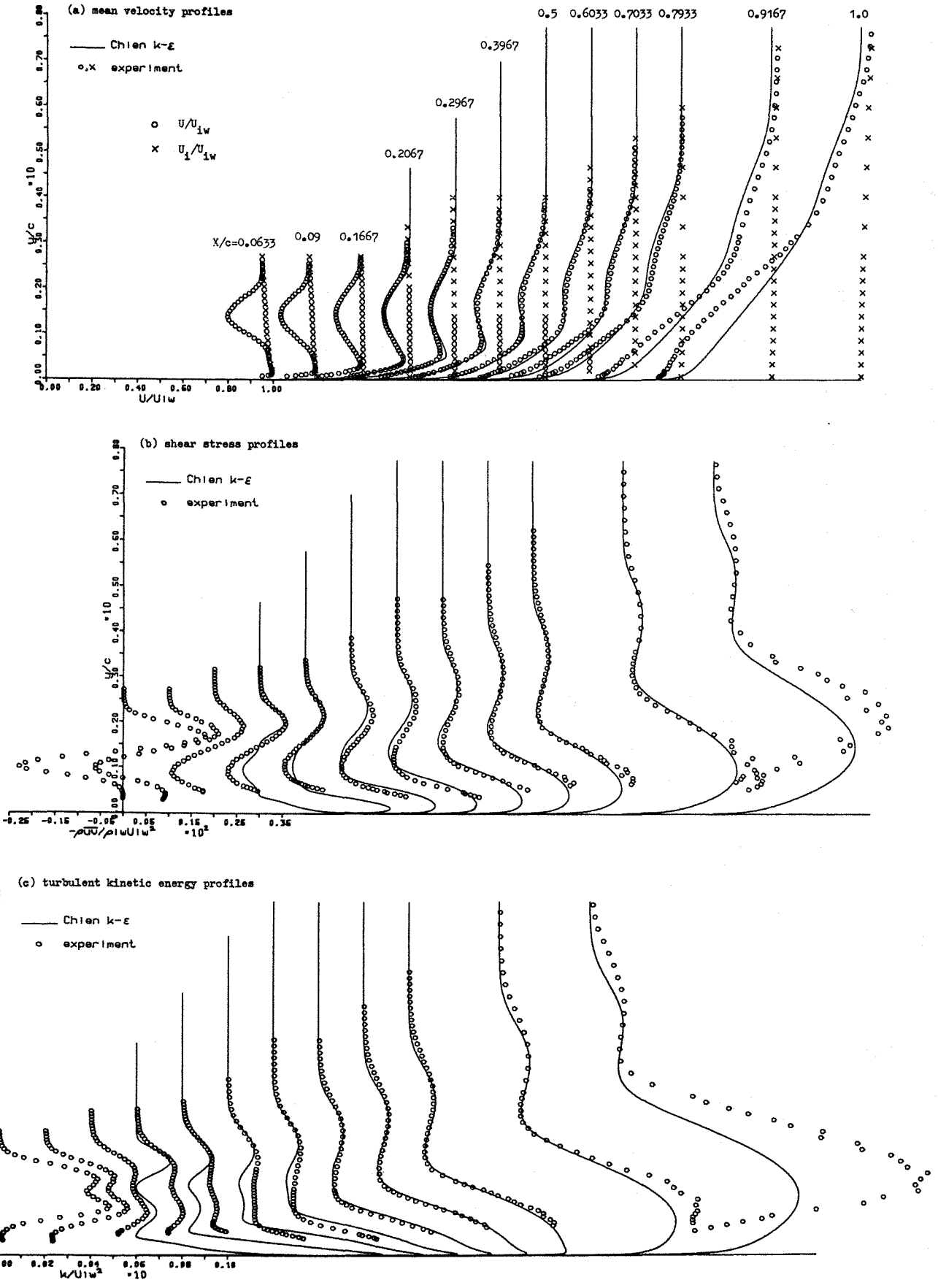
(a) mean velocity profiles
Chien k-ε
o,x experiment
o U/U_iw
x U_i/U_iw
X/c=0.0633
0.09
0.1667
0.2067
0.2967
0.3967
0.5
0.6033
0.7033
0.7933
0.9167
1.0
y/c *10
U/Uiw
(b) shear stress profiles
Chien k-ε
experiment
y/c *10
-ρUV/ρiwUiw² *10²
(c) turbulent kinetic energy profiles
Chien k-ε
experiment
y/c *10
k/Uiw² *10

FIGURE 8

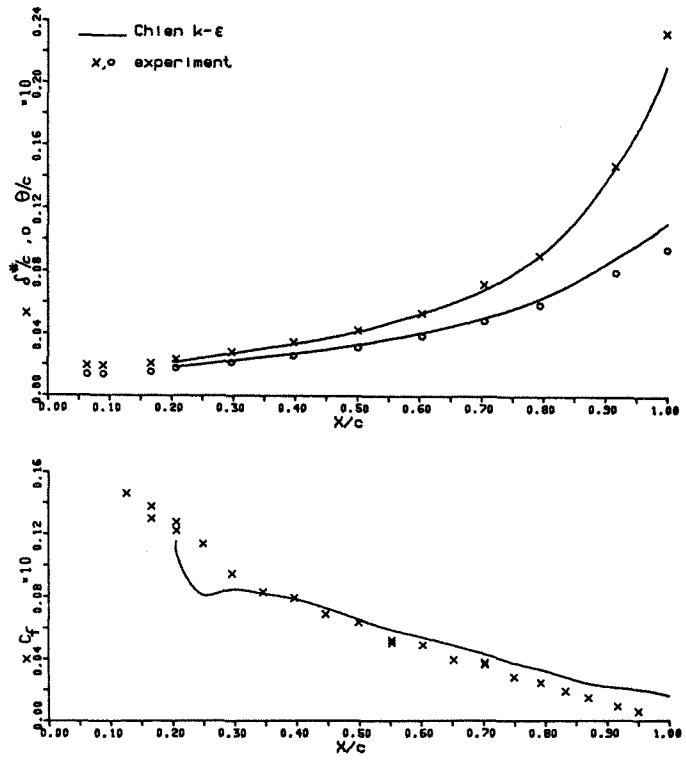

FIGURE 9

$$U^+ \equiv \frac{U}{U_\tau} = \frac{1}{\kappa} \ln(y^+) + C, \qquad (4)$$

with the usual constants $\kappa = 0.41$ and $C = 5.0$. U_τ is determined from the surface pitot probe measurements of the skin friction. Also shown in Figure 10 are the law-of-the-wake curve fits to the wall layer profiles for the first 8 stations. The law-of-the-wake profile used is a modified version of that due to Coles

$$\frac{U}{U_\tau} = 1 + \frac{1}{\kappa}\frac{U_\tau}{U_C}\left[\ln(y/y_c) - \Pi[1 + \cos(\pi y/y_c)]\right], \qquad (5)$$

where U_c and y_c are determined to ensure that $U = U_d$ and $\partial U/\partial y = 0$ at $y = y_d$. The wake parameter Π is evaluated using the implicit skin friction relation obtained by matching the law-of-the-wall to the law-of-the-wake

$$\frac{U_C}{U_\tau} = \frac{1}{\kappa}\ln(y_c U_\tau/\nu) + C + 2\frac{\Pi}{\kappa}, \qquad (6)$$

ν being the kinematic viscosity. Figure 10 indicates that the basic character of the wall boundary layer is unaffected by the mixing with the slat wake.

The mean velocity profiles for the two half-wake layers are replotted in Figure 11 in a form appropriate to a self-preserving wake of small velocity deficit. Two analytic curves are shown for comparison. The exponential profile

$$\frac{U_e - U}{U_e - U_W} = \exp\left[-\ln(2)\left(\frac{y - y_W}{L_O}\right)^2\right] \qquad (7)$$

is that obtained from a solution of the boundary layer equations assuming a constant eddy viscosity across the wake.[11] The cosine profile

$$\frac{U_e - U}{U_e - U_W} = \frac{1}{2}\left[1 + \cos\left(\frac{\pi}{2}\frac{y - y_W}{L_O}\right)\right] \qquad (8)$$

was found by Bario et al[7] to give closer agreement with their measurements. Similar expressions can be written for the inner half-wake layer, replacing U_e and L_o with U_d and L_i respectively. The profiles for the outer half-wake layer at different stations collapse well onto a unique curve. There is no definite mean velocity minimum in the profiles downstream of X/c = 0.6033, indicating that the outer half-wake layer has begun to merge with the wall layer. The self-similar behaviour of the inner half-wake layer breaks down for $(y_W - y) > 1.2\ L_i$ once the wake/boundary layer mixing commences. Figure 12 shows the half-widths and maximum velocity deficits of the two half-wake layers. Townsend[11] indicates that a wake of small velocity deficit, developing in a pressure gradient, can be self-preserving if $L_o \propto (x - x_o)$ and $\Delta U_o/U_e \approx$ constant. These conditions are satisfied by the outer half-wake layer for $X/c_s > 0.7$.

The mean velocity profiles for case (a) can be evaluated in the same manner, and lead to results consistent with those for the two-element aerofoil case. Reference 13 contains the data for case (b) in tabular form.

VI Turbulence Modelling

The eddy viscosity hypothesis relates the shear stress to the mean velocity gradient

$$-\overline{uv} = \nu_t\, \partial U/\partial y, \qquad (9)$$

and the eddy viscosity ν_t must be modelled. In the Prandtl mixing length approach, the eddy viscosity is given by

$$\nu_t = l_m^2 |\partial U/\partial y|, \qquad (10)$$

and l_m is assumed to have some universal form. The Prandtl-Kolmogorov length scale l is defined by basing the velocity scale of the eddy viscosity on the turbulent kinetic energy

$$\nu_t = \overline{q^2}^{\frac{1}{2}} l, \qquad (11)$$

where $\overline{q^2} = 2k$ and the usual constant of proportionality has been absorbed into l. Again, l is assumed to have a universal form and, in addition, a modelled turbulent kinetic energy transport equation must also be solved. Distributions of l_m and l have been derived from the mean flow and turbulence measurements. The results for the two experiments are similar, and so only the data for case (a) will be presented.

Figure 13 shows distributions of l_m and l for wall layer, scaled with y^*, the distance from the wall to the zero shear stress point. It should be noted that y^* does not coincide with the mean velocity maximum denoting the edge of the wall layer ($y^* < y_d$, and so there is a small region in which $-\overline{uv}$ and $\partial U/\partial y$ have opposite signs, in violation of the eddy viscosity hypothesis). The standard ramp function distributions of l_m and l, for an ordinary turbulent boundary layer, are also shown in the figure. The levels of both length scales are higher than the usual values once the

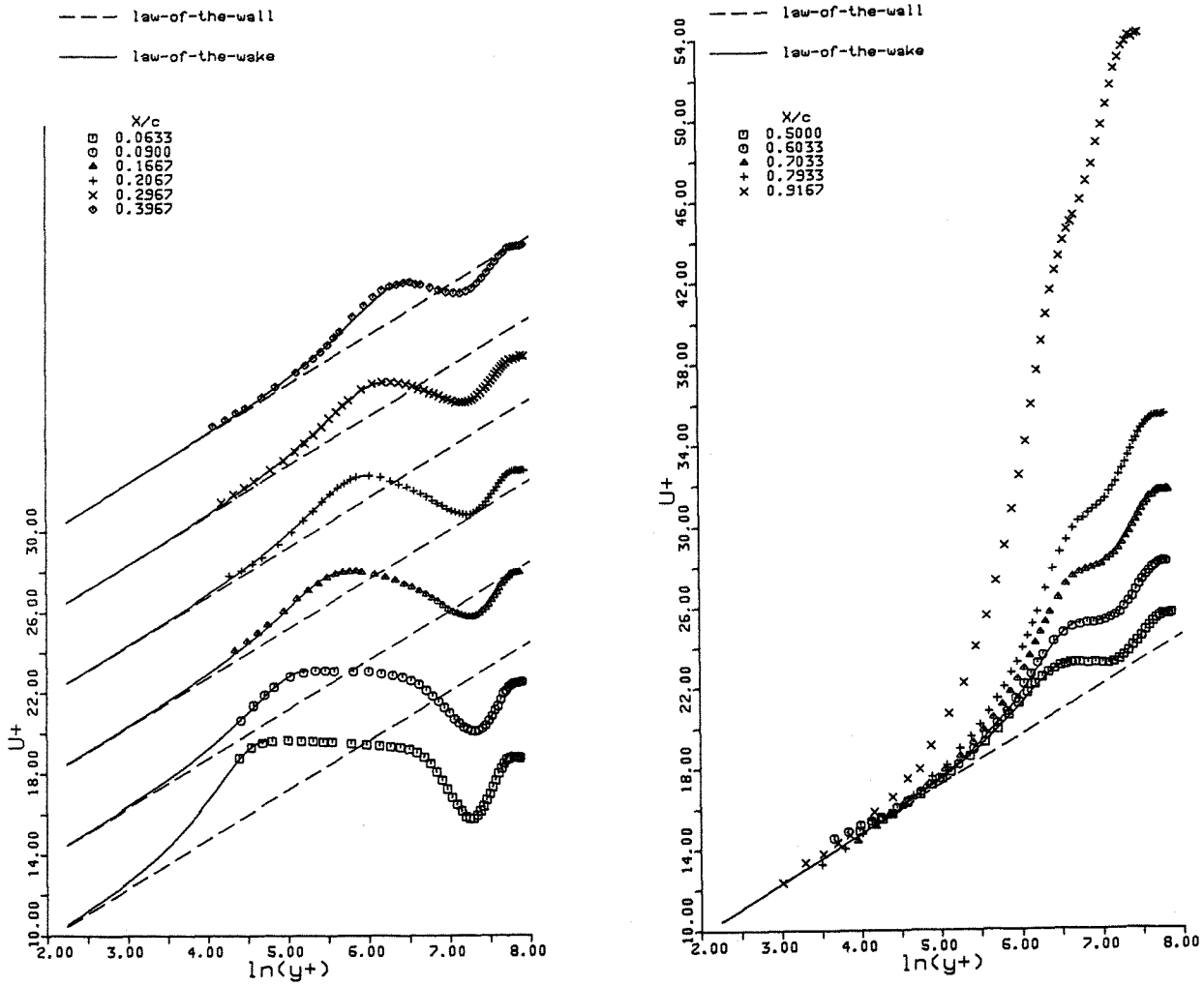

FIGURE 10

wake/boundary layer mixing commences.

The corresponding distributions of l_m and l for the two half-wake layers are shown in Figures 14 and 15. Both l_m and l scale well with L_o for the outer half-wake layer. However, there is no such scaling for the inner half-wake layer. Figure 16 shows the peak values of shear stress and turbulent kinetic energy for the outer half-wake layer, scaled with the maximum velocity deficit of the layer. The scaled peak shear stresses for both experiments are in good agreement with the relation $-\overline{uv} = 0.045\ \Delta U_o^2$ observed by Narasimha and Prabhu[14] in their equilibrium wake experiments. Townsend[11] indicates that both k_{max} and $-\overline{uv}_{max}$ should scale with ΔU_o^2 for self-preserving development of a wake. In the present experiments, $k_{max}/\Delta U_o^2$ becomes constant downstream of $x/c_s = 1.0$.

The mean flow and turbulence measurements show that the outer half-wake layer develops essentially as a free wake of small velocity deficit. The mean velocity profile attains a self-similar form, and both the shear stress and turbulent kinetic energy develop into equilibrium conditions, although k appears to lag behind $-\overline{uv}$. However, the inner half-wake layer displays no self-similar behaviour after the commencement of the wake/boundary layer mixing. Similarly, the turbulence levels in the outer region of the wall layer are substantially larger than in an ordinary turbulent boundary layer.

VII Calculation Methods

Integral calculation methods for wake/boundary layer mixing flows assume self-similar behaviour of the mean velocity profiles of the various layers. The present results indicate that any such behaviour breaks down in the inner half-wake layer. Also, the multi-layer representation cannot be used once the wake velocity minimum disappears. Thus, integral methods can be used to calculate only the initial stages of the wake/boundary layer mixing process. The alternative is to solve the mean flow equations in differential form, in conjunction with an explicit turbulence model. Again, the present results indicate that an algebraic turbulence model based on the multi-layer representation cannot be derived. A differential transport equation model of turbulence appears to be the minimum level of sophistication necessary to predict such flows.

Brune[15,9] used the popular k-ε two-equation turbulence model to predict a number of wake/boundary layer mixing flows. Adequate predictions

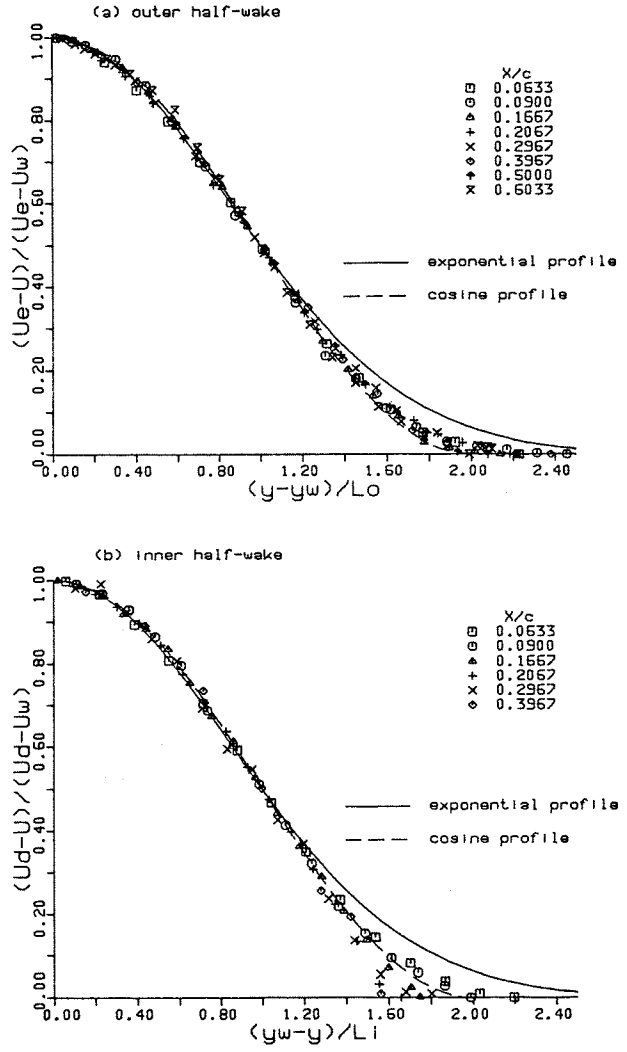

FIGURE 11

of mean flow quantities were obtained, but the levels of shear stress and turbulent kinetic energy in the wall layer were substantially overpredicted. The most likely cause of this discrepancy was the use of wall function near-wall boundary conditions, whereby the calculation was 'patched' to the law-of-the-wall at a point in the fully-turbulent region of the flow. The present approach was to use the Chien[16] low Reynolds number version of the k-ε model, allowing the calculation to extend right down to the wall. An existing finite-difference calculation method for boundary layer flows[17] was modified to allow the prediction of wake/boundary layer mixing flows. This involved changes only to the specified initial conditions. Initial shear stress profiles were generated using simple mixing length models and the multi-layer representation. The initial profile of turbulent kinetic energy was then generated using the structural parameter $a_1 = -\overline{uv}/k$, assumed to be constant across each of the layers.

Figures 4 and 5 show good agreement between calculations and measurements for case (a). The developments of the shear stress and turbulent kinetic energy profiles are particularly well predicted, despite the rather unrealistic initial

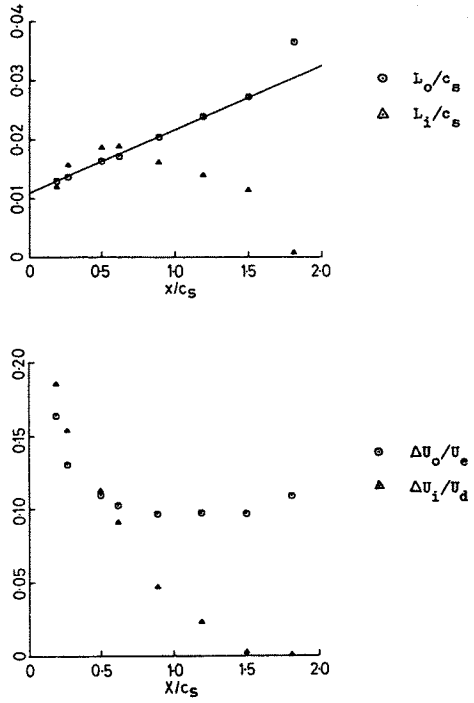

FIGURE 12

k profile. The calculation for case (b) begins at X/c = 0.2067, in a region with negligible variation of static pressure across the viscous layers (the calculation method does not allow for such variations). Again, Figures 8 and 9 show good agreement with the measured mean flow and turbulence quantities. The Chien k-ε model does, however, overpredict the skin friction levels in the adverse pressure gradient region downstream of X/c = 0.5. Patel et al[18] suggest that this is due to the behaviour of the near-wall damping functions used by Chien, as well as limitations with the parent high Reynolds number k-ε model. Nevertheless, the results are sufficiently encouraging to warrant further investigation of the k-ε turbulence model for application to wake/boundary layer mixing flows.

VIII Conclusions

Mean flow and turbulence measurements were made in two wake/boundary layer mixing flows. The measurements were used to investigate various aspects of the modelling of such flows. It was concluded that integral methods have only a limited applicability, due to the breakdown in any self-similar behaviour of the merging viscous layers. A differential boundary layer calculation method, together with the k-ε turbulence model, was used to successfully predict the present flows. It can be concluded that a two-equation turbulence model represents the minimum level of sophistication necessary to model these types of flows. However, the experiment involving a two-element aerofoil configuration indicated the presence of significant static pressure gradients normal to the surface. The effects of these gradients, on both the mean flow and turbulence development, need to be incorporated into the calculation method, to allow the prediction of the

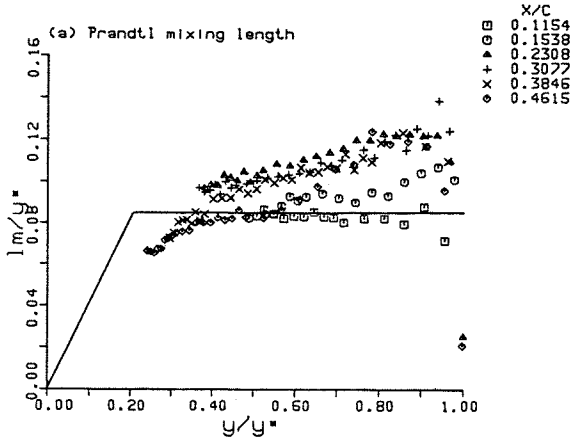

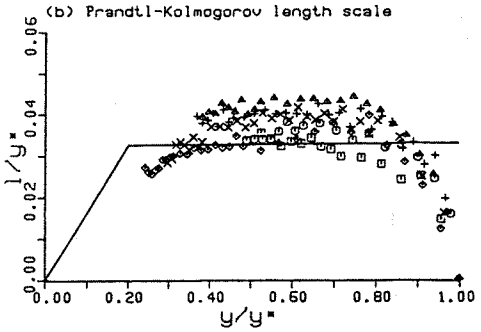

FIGURE 13

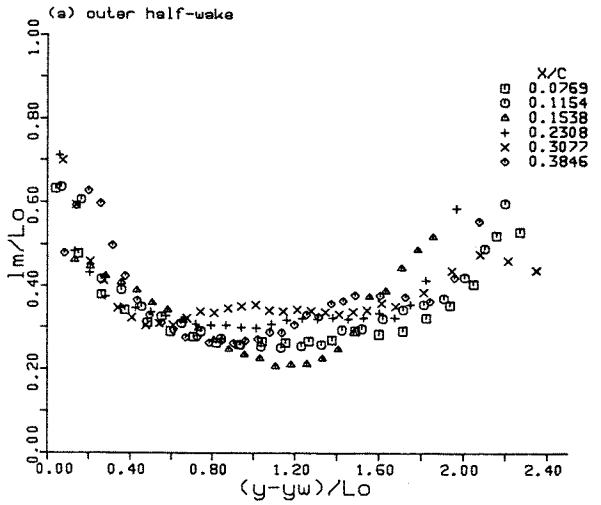

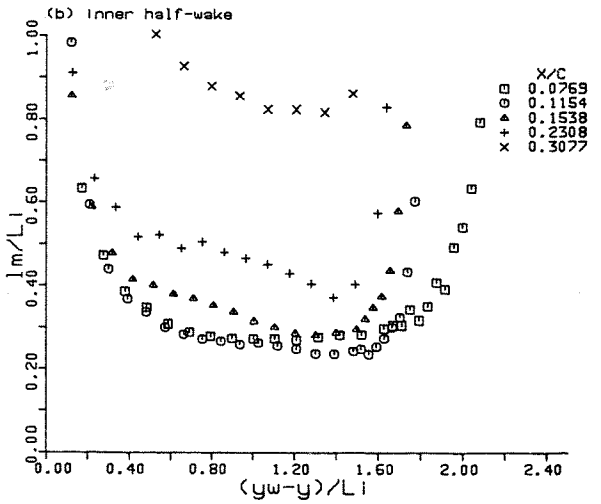

FIGURE 14

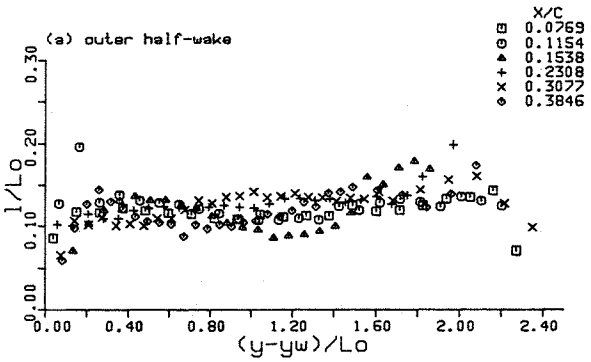

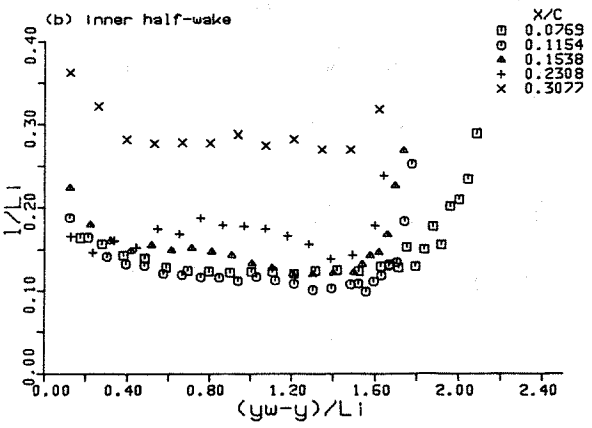

FIGURE 15

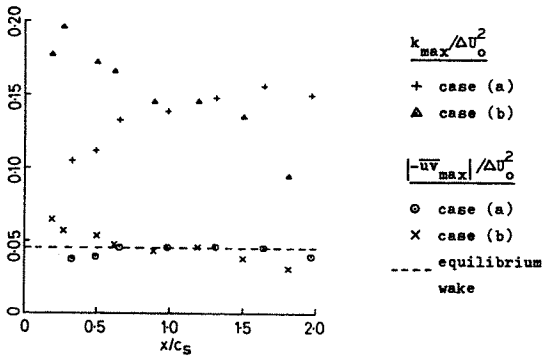

FIGURE 16

viscous flow around more practical high-lift configurations.

References

1 Petrov, A V, 'Some features of flow past slotted wings', RAE Library Translation 2050 (1980) from Uchenye Zapiski, TsAGI, 8, 6, pp 119/124 (1977).

2 Seetharam, H C and Wentz, W H, 'A low speed two-dimensional study of flow separation on the GA(W)-1 airfoil with 30% chord Fowler flap', NASA CR 2844 (1977).

3 Butter, D J, 'Recent progress on development and understanding of high lift systems', AGARD CPP 365, May 1984.

4 Irwin, H P A H, 'A calculation method for the two-dimensional turbulent flow over a slotted flap', ARC CP 1267 (1972).

5 Stevens, W A, Goradia, S H and Braden, J A, 'Mathematical model for two-dimensional multi-component airfoils in viscous flow', NASA CR 1843 (1971).

6 Pot, P J, 'A wake boundary layer mixing experiment', 2nd Symposium on Turbulent Shear Flows, Imperial College, London, 1979.

7 Bario, F, Charnay, G and Papailiou, K D, 'An experiment concerning the confluence of a wake and a boundary layer', Trans ASME, J Fluid Eng, Vol 104, No 19, 1982, pp 18/24.

8 Zhou, M D and Squire, L C, 'The interaction of a wake with a turbulent boundary layer', Aeronautical Journal, February 1985, pp 72/81.

9 Brune, G W and Sikavi, D A, 'Experimental investigation of the confluent boundary layer of a multi-element low speed airfoil', AIAA Paper 83-0566 (1983).

10 Johnston, L J, 'Two-dimensional turbulent wake/boundary layer mixing', PhD thesis, University of London, 1986.

11 Townsend, A A, 'The structure of turbulent shear flow', 2nd edition, 1976, Cambridge University Press.

12 Johnston, L J, 'Two-dimensional turbulent wake/boundary layer mixing - Part 1: constant pressure flow', Queen Mary College (University of London), Faculty of Engineering Paper QMC-EP-1070, September 1985.

13 Johnston, L J, 'Two-dimensional turbulent wake/boundary layer mixing - Part 2: a wing/leading edge slat configuration', Queen Mary College (University of London), Faculty of Engineering Paper QMC-EP-1071, September 1985.

14 Narasimha, R and Prabhu, A, 'Equilibrium and relaxation in turbulent wakes', J Fluid Mech, Vol 54, 1972, pp 1/17.

15 Brune, G W, 'Theoretical prediction of confluent boundary layers', 3rd Symposium on Turbulent Shear Flows, Davis, California, September 1981.

16 Chien, K-Y, 'Prediction of channel and boundary-layer flows with a low-Reynolds number turbulence model', AIAA J, Vol 20, No 1, 1982, pp 33/8.

17 Johnston, L J, 'A calculation method for two-dimensional wall-bounded turbulent flows', Aeronautical Journal, May 1986.

18 Patel, V C, Rodi, W and Scheuerer, G, 'Turbulence models for near-wall and low Reynolds number flows: a review', AIAA J, Vol 23, No 9, 1985, pp 1308/1319.